SAE International

2011-01-1660
Published
05/17/2011

Engine Fault Detection Using Vibration Signal Reconstruction in the Crank-Angle Domain

Ienkaran Arasaratnam and Saeid Habibi
McMaster University

Christopher Kelly, Tony J. Fountaine and Jimi Tjong
University of Windsor

doi:10.4271/2011-01-1660

ABSTRACT

Advanced engine test methods incorporate several different sensing and signal processing techniques for identifying and locating manufacturing or assembly defects of an engine. A successful engine test method therefore, requires advanced signal processing techniques. This paper introduces a novel signal processing technique to successfully detect a faulty internal combustion engine in a quantitative manner. Accelerometers are mounted on the cylinder head and lug surfaces while vibration signals are recorded during engine operation. Using the engine's cam angular position, the vibration signals are transformed from the time domain to the crank-angle domain. At the heart of the transformation lies interpolation. In this paper, linear, cubic spline and sinc interpolation methods are demonstrated for reconstructing vibration signals in the crank-angle domain. Finally, the ensemble-averaged mean squared-error criterion is introduced as the fault-detection metric to determine whether the engine under test is faulty or not. The proposed method is cost effective, non-intrusive and non-destructive. Moreover, the results have shown the crank-angle domain analysis using sinc interpolation for signal reconstruction to be more precise than that using linear or cubic spline interpolation. This improved precision enables better fault detection with a more accurate measure of the severity of the fault condition.

INTRODUCTION

One of the main objectives of every manufacturer is to cost effectively achieve high productivity while increasing customer satisfaction and product reliability. In a production environment, in-process test systems are used to check the engine as it is being assembled to ensure that components are properly installed and functioning before the assembly process is complete [31, 32]. An in-process test system is always preferred to testing products upon completion of the entire assembly because it greatly increases productivity by reducing downtime and scrap cost. After the engine is completely assembled engine manufactures have been known to use either ‘cold’ or ‘hot test’ methods for many years in an attempt to detect and diagnose manufacturing and assembly defects [1, 10, 12, 15, 21, 25, 27]. These test stands provide a more detailed check of the engine as some defects are detectable only after an engine is completely assembled and subject to certain operating conditions. For example, some defects show up when the engine is running at a specific speed, load and oil temperature.

Engine defects can be located by monitoring:

- torque;
- wire harness signals from engine sensors and actuators;
- sound measurements;
- pressure measurements collected from fuel, intake/exhaust manifolds, crankcase and in-cylinder; and
- vibration signals.

Of these measurements, vibration signals are widely used in the manufacturing industry. The acquisition of vibration signals is relatively inexpensive and does not require engine tear-down. Above all, it is also possible to infer various engine defects by post-processing vibration signals. All machines vibrate because they are mechanical systems with moving components and are comprised of an elastic system

that oscillates in response to excitations. When a machine malfunctions, it causes the excitation forces to vary and thus changes its system characteristics and hence the vibration signature of the system. This change can be detected and distinguished from a normal condition using spectral and vibration analysis. In the past, vibration analysis methods have been applied to reciprocating machines, gearboxes [19], transmissions [29], and also a few applications involving internal combustion engines [4, 11, 27, 28].

Noise and vibration of a faulty combustion engine are generated from the following sources [2, 8]:

• *Impulsive impact* among components due to incorrect clearance between valve train, gears, connecting rods, pistons, bearings etc.

• *Imbalance* in rotating components of the engine such as crankshaft, camshaft(s), balance shaft and or gears.

• *Abnormal combustion* due to incorrect ignition/injection timing, knock, detonation, incorrect valve opening etc.

• *Manufacturing defects* due to improper part orientation, missed oil galleries, fasteners, bearings or other components

• *Poor power transfer* when the translational motion is converted into rotational motion and vice versa; For example, a few causes for this phenomenon are defective gears, eccentric gear orientation and poor cam shapes.

The main motivation of this paper is to accurately predict whether the engine is faulty by analyzing vibration signals. To accomplish this task, accelerometers are mounted on the engine and the vibration signals are recorded during engine operation. With the aid of a tacho (reference) signal, the measurements are transformed to the crank angle (CA) domain where the results are compared with the baseline data collected from a 'pass' engine in terms of the ensemble-averaged mean squared-error criterion. At the heart of the domain transformation lies interpolation. The reasons for transferring to the CA domain will be discussed later in this paper. This paper demonstrates the following:

• The (truncated/windowed) sinc interpolation method is used for registering vibration signals in the CA domain.

• It is demonstrated that sinc interpolation significantly outperforms both linear and cubic spline interpolation.

• It is concluded that truncated sinc interpolation and windowed sinc interpolation perform equally for the vibration signal registration problem.

The paper is organized as follows: First, the problem statement is presented while the engine setup is explained. Next, vibration signal analysis in the CA domain is presented. This section discusses different interpolation methods with a special emphasis on the application of the sinc interpolation method. Finally, the proposed method is applied to engine fault detection and the results are interpreted using the ensemble-averaged mean-squared error (EA-MSE) criterion, before the final remarks are presented.

CONTEXT AND SIGNAL ACQUISITION

In this section, the fault condition, test set up and test conditions are briefly described as context for this paper. The test presented in the paper was performed on a naturally aspirated four stroke, eight cylinder engine. The engine under consideration was exhibiting abnormal noise which could be heard above the normal operating noise of the same engine model. Although such abnormal noise levels allow us to judge the engine condition, the judgment is subjective and does not necessarily agree with the judgment of another person, especially in the case of fault conditions on the border line of acceptability. Therefore, the problem this posed was to classify the engine as 'pass' or 'fail' in a quantitative manner.

To solve this problem, vibration measurements were used. Before starting to acquire vibration data, the engine was warmed up until the oil and coolant temperatures reached normal operating conditions. A total of eight charge-type piezoelectric accelerometers were mounted on the engine so that they were located perpendicular to the crankshaft axis as shown in Figures 1 and 2. Four of them were mounted on the cylinder head located at each corner of the cylinder head, namely, right front head (RFH), right rear head (RRH), left front head (LFH) and left rear head (LRH). The purpose of these sensors was to capture vibration emanating from the upper part of the engine (head). This vibration may be due to valvetrain components such as cam caps, lash adjusters, phasers or oil dynamics, to name a few (see Figure 1(a)). The remaining four accelerometers were mounted on the cylinder block manufacturing lugs located at each corner of the cylinder block, namely, right front lug (RFL), right rear lug (RRL), left front lug (LFL) and left rear lug (LRL). These sensors focused on capturing noise which would emanate from the lower parts of the engine such as pistons, rings, crankshaft gears, seals, etc. The reader may consult [23] for optimal positioning of these accelerometers. All accelerometers were calibrated before their use. As shown in Figure 3, the engine was equipped with a data acquisition system having a built-in signal conditioner. The analog vibration signal was digitized using a 16-bit analog-to-digital converter while the system used a sampling rate of 32768Hz/ channel. The vibration signals were collected from the accelerometers for four seconds while the engine was coupled to a dynamometer and running at 2000 rpm with wide open throttle (WOT). The corresponding brake torque generated by the test engine in this condition was 484 Nm. Four seconds of data at 2000 rpm provides approximately 66 entire engine cycles for data analysis (One engine cycle is equivalent to

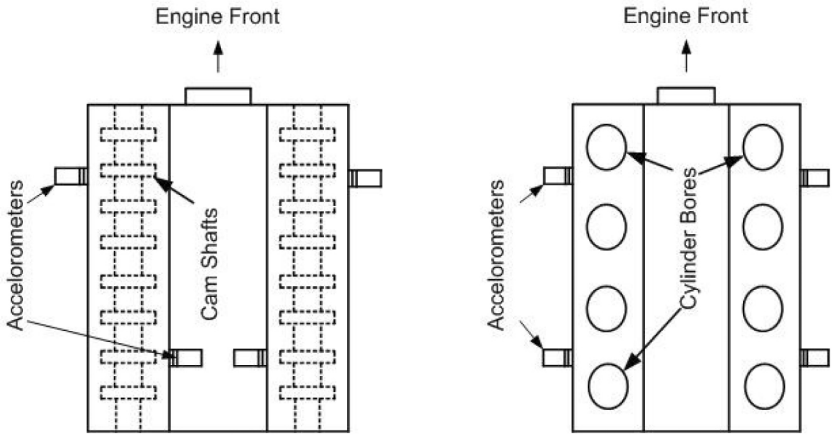

Figure 1. Accelerometer positions from engine top views (a) head positions (b) block positions

one complete revolution of the camshaft or two complete revolutions of the crankshaft).

The camshaft sensor, which is also known as the Cylinder IDentification (CID) sensor, is used as a reference to time the sequential fuel injection and spark events [6]. The signal from the CID sensor is a result of the changing magnetic field as the camshaft tabs rotates past a magnetic pickup. It can be either a digital square wave (Hall-effect sensor) or in this particular case a sine wave because the sensor is of the Variable Reluctance Type (VRS) [22]. The Engine Control Unit (ECU) needs to see the signal when the engine is started for its reference. During the data acquisition of vibration signals, the CID signal was also recorded because it provided a reference to the entire engine cycle. Note that it may lose synchronicity of about 0-30 CA degrees due to the Variable Cam Timing (VCT) mechanism of the engine. Figure 4 shows the CID signal and the vibration response recorded by the data acquisition system; the segment in between the two dotted lines corresponds to data for a single engine cycle at 2000 RPM.

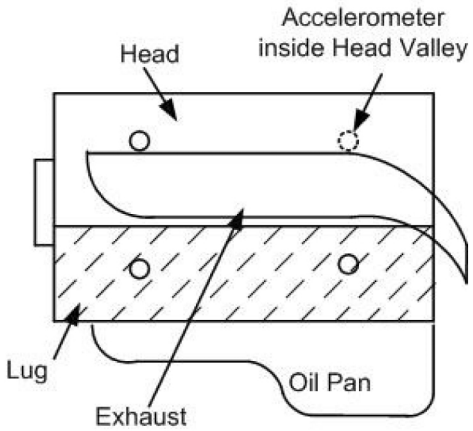

Figure 2. Accelerometer positions from engine side view

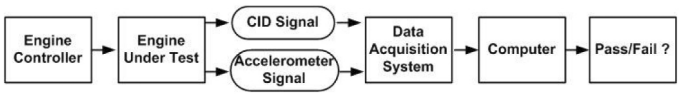

Figure 3. Test set-up

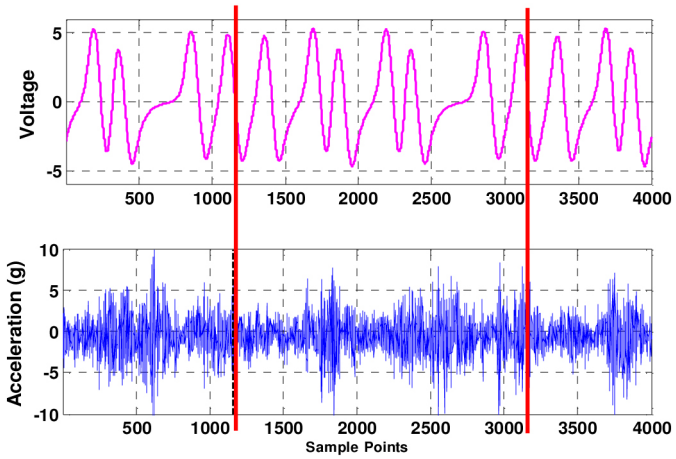

Figure 4. Time History: (a) Reference CID Signal (b) Raw Vibration Signal Acquired from the Right Rear Lug Location.

SIGNAL ANALYSIS

Signal analysis can be performed in the time domain or crank-angle domain as follows.

TIME DOMAIN ANALYSIS

The time domain analysis is simple and quite straightforward for fault detection. In this method, a number of statistical parameters related to the time domain vibration signal are examined to detect the presence of any defects. These parameters include standard deviation, root mean square (RMS), crest factor, skewness and kurtosis [8]. By comparing these statistical parameters of the baseline engine, the

presence of a defect and its degree of severity are determined. This approach has been widely used in detecting bearing damages [13, 17]. However, the analysis of engine noise and vibration in the time domain is seldom performed for a number of reasons:

• Vibration signals registered in the time domain using a fixed sampling rate do not properly account for engine speed variations. Even when the engine speed is set to a specific rpm, in reality, the speed fluctuates from cycle to cycle or even within an engine cycle. Some of the main reasons for the speed fluctuations can be due to mechanical and electrical loads and temperatures that are present [26]. The engine speed is largely dependant on the torque. Because the internal combustion engine does not continuously produce torque (it has torque pulses with each power stroke), the speed can be expected to have some fluctuations. To better understand the relationship of the speed and torque, the reader may refer to [5, 16].

• Internal combustion engines operate in a cyclic manner; the time domain analysis is not quite effective at revealing abnormalities of (semi-)periodic signals (For example, in Figure 4, there are no particular features that would aid in classifying the engine as pass or fail).

• Better noise reduction requires substantially long signals and many ensemble averages.

To get around these shortcomings, a unique technique using the already present engine CID sensor as opposed to installing a crankshaft encoder is presented. Sinc interpolation is used to improve the conversion from the time to the CA domain.

CRANK-ANGLE DOMAIN ANALYSIS

The CA domain analysis is useful for correlating any observed signal abnormalities with specific mechanical events such as [2]:

• Piston stroke position/slap due to (intake, compression, combustion or exhaust)

• Valve events (open/closing of intake/exhaust valves)

• Injection/Ignition events

• Cylinder pressure

• Combustion events such as knock

In order to transform a time-domain signal into a CA domain signal, a synchronized acquisition of vibration measurements with a crankshaft (encoder) or camshaft position CID [6] is required. For data collected in this paper the signal from the CID sensor is acquired. For the engine being studied the CID generates a unique signal using seven sinusoidal pulses for each engine cycle (720°); those pulses are separated in the CA domain as follows 90°, 120°, 60°, 120°, 60°, 180°, 90° (see Figure 5). Engine speed although varying slightly is assumed to be constant between each of the tabs.

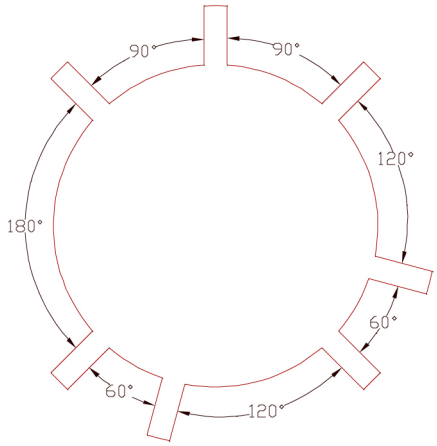

Figure 5. Cam Tabs for CID Pulse generation separation in the CA domain.

In general, top-dead-center (TDC) of the first cylinder or the crank wheel's angular position of zero is located some engine-specific degrees offset to the zero crossing of the first pulse of the CID signal crankshaft position. The next step is to resample the time domain signal captured in each engine cycle so that the new set of samples in each engine cycle meets the following two conditions:

• The new samples have a constant crank angle distance

• The number of new samples per engine cycle is constant for all engine cycles

To this end, interpolation is applied. Various interpolation methods have been described especially in the computed order tracking literature in varying levels of details[9, 24, 30]. Specifically, this paper focuses on sinc interpolation as described next.

SINC INTERPOLATION METHOD

The sinc function is defined by

$$\operatorname{sinc}(t) = \begin{cases} \dfrac{\sin(\pi t)}{\pi t} & t \neq 0 \\ 1 & t = 0 \end{cases} \qquad (1)$$

This function is the continuous inverse Fourier transform of the rectangular pulse of width 2\pi and height unity:

$$\operatorname{sinc}(t) = \frac{1}{2\pi}\int_{-\pi}^{\pi} \exp(j\omega t)\, d\omega \qquad (2)$$

Hence, the sinc function can be considered as the 'ideal' low-pass filter impulse response. Moreover, any band limited

signal *x(t)* can be reconstructed from its infinite number of samples at integer spacings:

$$\tilde{x}(t) = \sum_{k=-\infty}^{\infty} x[k]\,\mathrm{sinc}\left(\frac{t - kt_s}{t_s}\right) \qquad (3)$$

where t_s is the sampling interval. From (3), $\tilde{x}(t)$ equals the superposition of shifted version of sinc(t/t_s) weighted by the samples x[k]. Equivalently, at time $t = nt_s$, (3) boils down to an equation of the convolution form:

$$\tilde{x}[n] = \sum_{k=-\infty}^{\infty} x[k]\,\mathrm{sinc}([n-k]) = \{x[k]\} * \{\mathrm{sinc}[k]\} \qquad (4)$$

where * denotes the convolution operator.

Unfortunately, the sinc-based reconstruction is unrealistic from practical viewpoint because the summation in equation (3) extends from minus infinity to infinity. Therefore, it must be truncated somewhere to be of practical use. For signals that are not band limited, the truncated-sinc interpolation method provides the least mean squared-error signal reconstruction. The truncated-sinc interpolation method is used as the yardstick by which all other interpolations are evaluated in their ability to reconstruct band-limited signals.

For example, given a sampled signal x[k] = [1.5, 2, 4, 1.5, 2.5] that is zero outside the given time interval, let the signal be sampled at exactly the Nyquist frequency. As can be seen from Figure 6, at each sampling time k, the sample x[k] is replaced by a sinc function whose peak equals x[k] and zero-crossing occur at all other sampling instants.

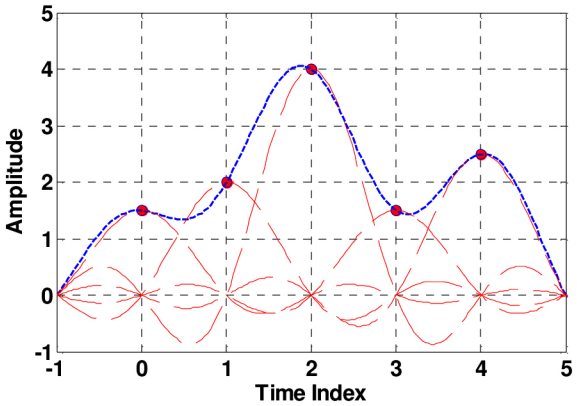

Figure 6. Reconstructed Signal as a Weighted Sum of Shifted sinc Functions.

WINDOWED SINC INTERPOLATION METHOD

The windowed sinc interpolation method applies the windowed sinc function, which may be expressed as follows:

$$h(t) = \frac{\cos\left(\frac{\pi\beta t}{t_s}\right)}{1 - 4\left(\frac{\beta^2 t}{t_s}\right)} \sin c\left(\frac{t}{t_s}\right) \qquad (5)$$

where $0 \le \beta < 1$ is the roll-off factor. In digital data communication literature, Equation (5) is also called the 'raised-cosine function'. Figure 7 illustrates how the windowed sinc function varies with β. For $\beta = 0$, the windowed sinc function reduces to the sinc function. As β increases, it decays rapidly and the oscillations on both sides of the origin quickly tend towards zero. For this reason, the windowed sinc interpolation method requires fewer past and future samples than the truncated-sinc interpolation method. As β tends to unity, it approximates the linear interpolation method. For the purpose of re-sampling, typically, the windowed sinc interpolation method using $\beta = 0.22$, is used, which is roughly equivalent to the Hann window. In terms of computational complexity, the windowed sinc interpolation method is more expensive than the truncated sinc interpolation method due to the scaling factor.

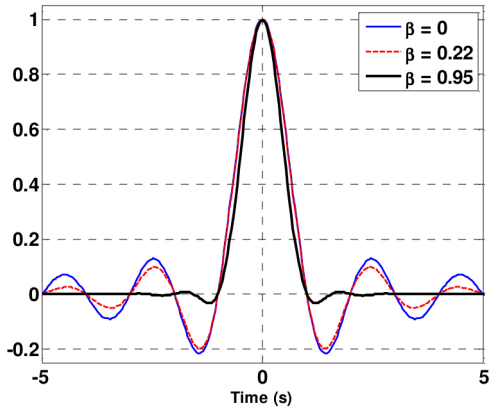

Figure 7. Windowed Sinc: Change of Oscillation with Increasing Roll-off Factor, β.

MOTIVATING NUMERICAL EXAMPLE

The following is an example which provides experimental evidence that when preservation of information contained in original data is required, the sinc-interpolation method outperforms other traditional interpolation methods such as linear and cubic-spline interpolation. Although the linear interpolation method is the most common and fastest, it is typically the least accurate. The linear interpolation method is also the simplest form of interpolation, as it simply connects two adjacent data points with a straight line, and uses the

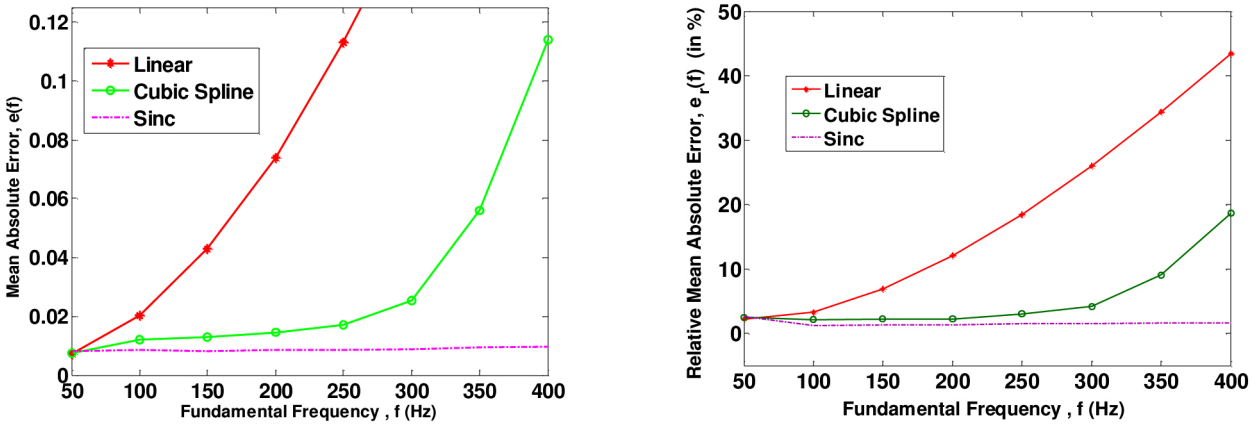

Figure 8. Change of MAE and RMAE with Increasing Fundamental Oscillation Frequency (f)

equation of that line segment to determine the desired value. On the other hand, the cubic spline interpolation method is often superior to the linear interpolation method since cubic splines are derived purely from smoothness conditions, where the second derivative of the interpellant must be continuous across the interpolating points [7].

For comparison purposes, these interpolation methods are demonstrated in reconstructing an oscillating transient signal of the form:

$$x(t) = \exp(-\alpha_1 t)\sin(2\pi f t + \phi) + \exp(-\alpha_2 t)\sin(4\pi f t) \tag{6}$$

where decaying constants $\alpha_1 = 20$ and $\alpha_2 = 4$; $\phi = \tan^{-1}\left(\frac{\alpha_1}{2\pi f}\right)$. Oscillating transients are often used to represent the shock response of a spring-mass-dashpot system. For this example, assume a data set of which is 0.5s long sampled uniformly providing 512 points. This signal was reconstructed using an up sampling factor of 1.5, which resulted in 768 new samples after interpolation. Four different interpolation methods, namely, linear, (piecewise) cubic spline, truncated sinc and windowed sinc were tested. For comparison of the interpolation methods, the mean absolute error (MAE, $e(.)$) and the relative mean absolute error (RMAE, e_r (.)) are defined as follows:

$$e(f) = \frac{1}{K}\sum_{k=1}^{K} |\hat{x}[k] - x[k]| \tag{7a}$$

$$e_r(f) = \frac{1}{K}\sum_{k=1}^{K} \frac{|\hat{x}[k] - x[k]|}{|x[k]|} \times 100 \tag{7b}$$

where $\hat{x}[k]$ is the estimate of the true sample value $x[k]$ at the time index k and the total number of interpolating points k = 768. For this example, the fundamental oscillation frequency (f) is increased from 200Hz to 500Hz in a step size of 50Hz. It was found that the results from the truncated sinc and windowed sinc interpolation were nearly identical and overlapping. For this reason the results depicted in Figures 8 and 9 show truncated and windowed sinc interpolation as 'sinc'. Figure 8 also shows both the MAE and the RMAE of the sinc interpolator is the smallest and remains almost constant compared to the other two methods. As the signal content (or f) increases, unlike the sinc interpolator, the error magnitudes of the linear and cubic spline interpolators grow exponentially.

Figure 9 shows the amplitude spectrum of the original signal and the reconstructed ones when f = 200Hz. The amplitude spectrum of the true transient consists of two peaks around f = 200Hz and 400Hz, which correspond to the fundamental frequencies of oscillations of transients. As can be seen from Figure 9, unlike the sinc interpolator, the other two interpolators introduce harmonic distortions at high frequencies (above 600Hz), which is quite undesirable. The misrepresentation of the original spectrum can be attributed to the large deviation of the reconstructed signal from the true signal. This misrepresentation should be expected for the following reason: Consider, for example, the linear interpolation. It reconstructs the signal at interpolating points by connecting two available adjacent points by a line as explained earlier. In the frequency domain, the construction of abruptly changing slopes leads to the introduction of high frequency components.

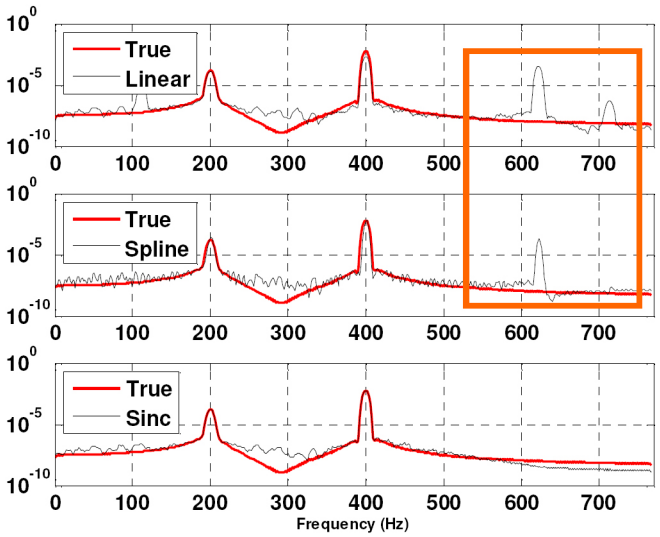

Figure 9. Deviation from the Original Amplitude Spectrum: Original Transient (thick line) and the Transient Reconstructed using Three Different Interpolation Methods (thin lines). The Boxed Region Shows the Misrepresentation of the True Spectrum

SIGNAL RECONSTRUCTION VIA INTERPOLATION

Vibration signal reconstruction in the CA domain is a five-step procedure as follows.

• Determine the falling-edge locations of the CID signal in terms of sampling-time indexes just after its values go below zero as shown in Figure 10-(a).

• Match the falling-edge locations of the CID signal to the crank shafts angular segment based on the information about the number of samples/cycle and the number samples per interval defined by adjacent falling edges. For the given example, the CID sensor generates seven pulses per two revolutions of the crank shaft, which results in the following angular segments in the CA domain (90°, 120°, 60°, 120°, 60°, 180°, and 90°). See Figure 5 and Figure 10-(c). It is assumed that the engine speed remains constant in the time intervals defined by the crankshaft's angular segments.

• Let the angular resolution for re-sampling in the CA domain be $\Delta\theta$. Compute the number of new samples required for every crankshaft angular segment. For the case of $\Delta\theta = 0.1°$, 7200 (= 720°/0.1°) samples/engine cycle can be obtained.

• Given the set of (old) time-domain samples and the engines crank shaft angular segments (Figure 10-(a)), compute the new sample values using interpolation (Figure 10-(d)).

• Shift the new samples obtained for every engine cycle so that they are aligned with the top-dead center of the first cylinder.

This five-step procedure was applied to the vibration signal collected from the test engine described in the context and signal acquisition section.

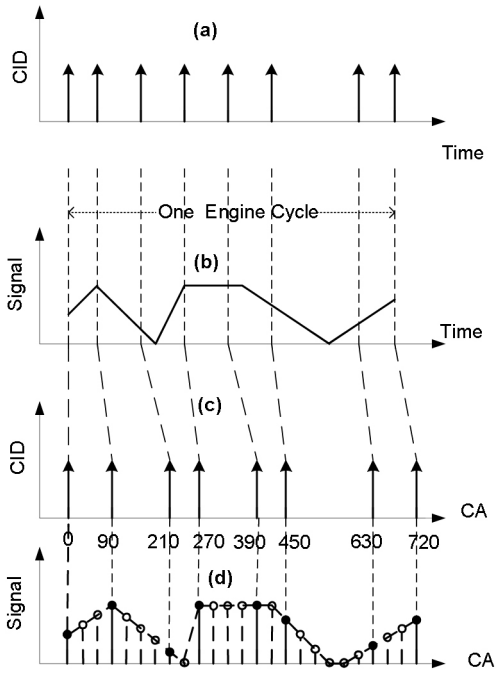

Figure 10. Reconstruction of vibration signal in the CA domain: (a) CID signal in the time domain (falling edges of the CID signal are depicted by arrows); (b) Vibration signal captured in the time domain; (c) falling edges of the CID signal in the CA domain; (d) Vibration signal in the CA domain

EXPERIMENTAL RESULTS & INTERPRETATION

Similar to the vibration signal in the time domain, simply viewing the vibration signal in the CA domain would reveal little information about the fault condition. However, unlike the time signal, because every engine cycle in the CA domain consists of the same number of samples, it allows us to compute ensemble-based statistics. For our study, the ensemble-averaged mean squared error (EA-MSE) is used, the computation of which includes three steps:

• Calculate the ensemble average

$$\bar{x}_i = \frac{1}{N}\sum_{j=1}^{N} x_{i,j} \qquad (8)$$

where N is the number of cycles; $x_{i,j}$ denotes the amplitude of the j-th cycle (j = 1 … N) at i-th crank angle (i = 0, $\Delta\theta$, … 720°)

• Calculate the instantaneous mean squared error

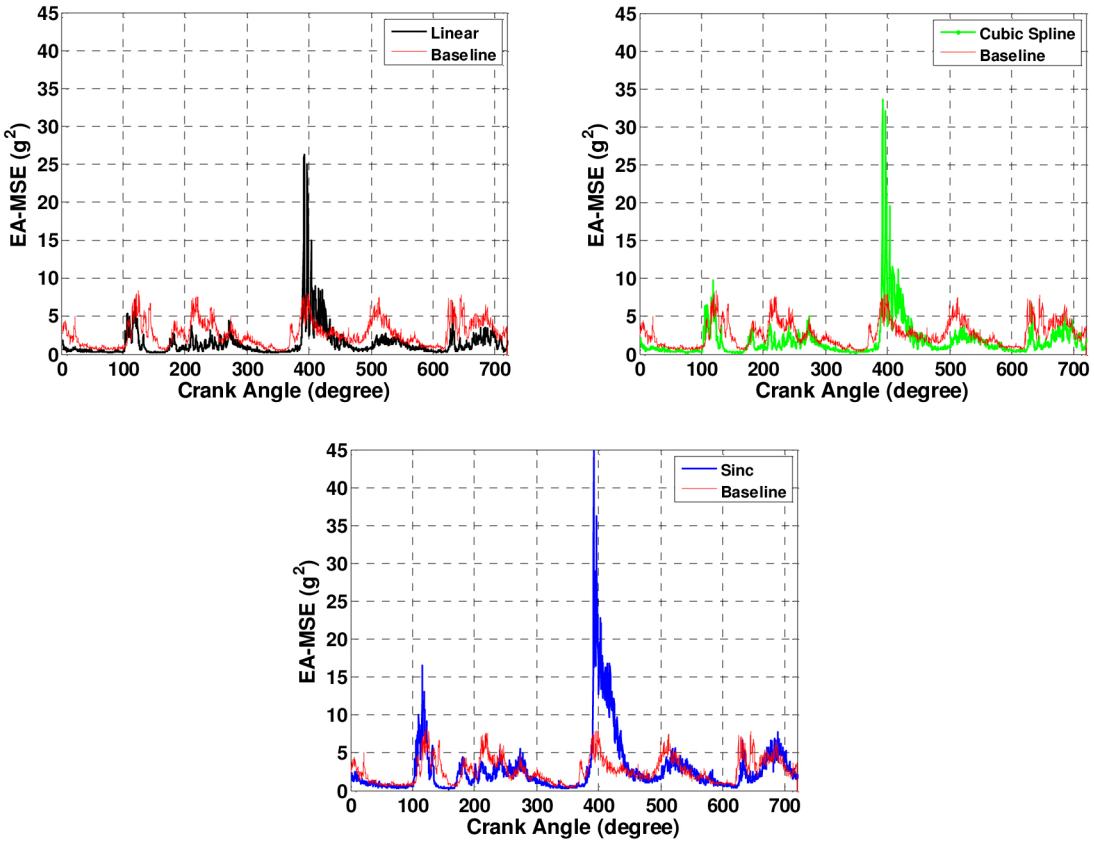

Figure 11. This EA-MSE (averaged over 64 cycles) of Three Interpolation Methods s in the Crank Angle Domain.

$$e_{i,j} = \left(x_{i,j} - \bar{x}_i\right)^2 \tag{9}$$

• Calculate the EA-MSE

$$e_i = \frac{1}{N}\sum_{j=1}^{N} e_{i,j} = \frac{1}{N}\sum_{j=1}^{N} x_{i,j}^2 - \bar{x}_i^2 \tag{10}$$

The signal due to a fault condition produces more power than the signal due to a normal condition. The EA-MSE can be viewed as the average power of the signal. Moreover, because the EA-MSE only attenuates signal amplitudes of normal events, the signal amplitudes of irregular events become more visible. Note that a crude form of ensemble averages has been in use for over 50 years for fault diagnosis in cold and hot stands.

Observations: Figures 11(a)-11 (c) show the EA-MSE computed on the RRL accelerometer data acquired from a 'pass' engine (denoted by the term 'baseline' in the legend area) and the engine described in context and signal acquisition section using three different interpolators. Again, the results of the truncated and windowed sinc interpolators were nearly identical. As such, they are represented as 'sinc' in Figure 11(c). As compared to the linear and cubic-spline interpolators, the sinc interpolator has a significantly taller impulse-like spike around 400° CA. The taller spike can be attributed to higher energy content due to abnormal audible noise. The overlay plot in Figure 12 allows us to examine this observation in fine detail. The accurate height information of the abnormal spike enables us to reliably predict whether the engine is faulty or not. Moreover, to a certain extent, the degree of severity of the fault condition can be reliably inferred.

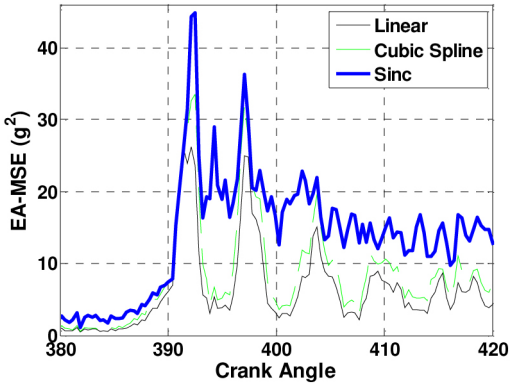

Figure 12. Detailed View of the EA-MSE Plot around 400° Crank Angle

CONCLUSIONS

This paper demonstrated that the sinc interpolation method is capable of reconstructing signals in the CA domain more accurately. Because the truncated-sinc interpolators and the windowed-sinc interpolators achieve the same performance in terms of reconstruction accuracy, the truncated sinc interpolation method may be preferred for its reduced computational cost. The (windowed/truncated) sinc interpolation method is easy to implement (see Appendix). Note that the sinc interpolation method has the following limitations although they may not be relevant to the fault detection problem:

- It is not the optimal interpolation method due to truncation.
- Because the sinc function varies smoothly, it cannot properly reconstruct a discontinuous signal at the discontinuities. To be more specific, it can be applied only to signals band limited by Nyquist frequency
- Unlike the linear and cubic spline interpolation methods, the sinc interpolation method cannot be implemented online; it requires all the past and future samples. The use of a sinc interpolator is therefore, appropriate for post analysis.

The CA domain analysis helps to relate the abnormal spike to a particular mechanical event of the combustion cycle and thus the piston position. Depending on where the accelerometer related to this abnormal spike is mounted, the analysis further aids in focusing on a specific portion of the engine. However, to be definitive about the specific fault type, more complex post processing techniques such as order tracking, spectrum analysis, wavelets, principal component analysis and subspace methods [18] may be required. The CA domain analysis technique described herein can be easily extended to transform acoustic and in-cylinder pressure signals into the CA domain, which may in turn aid in the detection of piston slap [2], valve events [2], improper manufacturing/assembly of the engine [8], knock [14,20], auto-ignition combustion and misfires [3], the estimation of combustion metrics such as torque and indicated mean effective pressure [3], etc. Moreover, because the CID signal aids to convert the signal in the crank-angle domain without the need for an external encoder, the CA domain analysis reported in this paper may be implemented in a vehicle for on-board fault diagnosis.

REFERENCES

1. Alvey, A. and Jay, G., "Application of NVH Techniques to Engine Production Line Test," SAE Technical Paper 2005-01-2452, 2005, doi:10.4271/2005-01-2452.

2. Antoni, J., Daniere, J., Guillet, F., "Effective Vibration Analysis of IC Engines Using Cyclostationarity. Part I - A Methodology for Condition Monitoring", Journal of Sound and Vibration, 257(5), 815-837.

3. Ball, J., Bowe, M., Stone, C., and McFadden, P., "Torque Estimation and Misfire Detection using Block Angular Acceleration," SAE Technical Paper 2000-01-0560, 2000, doi:10.4271/2000-01-0560.

4. Chandroth, G.O., Sharkey, A.J.C., Sharkey, N.E., "Cylinder pressures and vibration in internal combustion engine condition monitoring", Proceedings of Comadem 99, Sunderland, UK, July, 1999.

5. Christen, U., Vantine, K., and Collings, N., "Event-Based Mean-Value Modeling of DI Diesel Engines for Controller Design," SAE Technical Paper 2001-01-1242, 2001, doi: 10.4271/2001-01-1242.

6. Daws, M.C., "Assessment of the impact of camshaft machining inputs on valvetrain sound quality using vibration analysis," Masters Thesis, University of Windsor, 2002.

7. de Boor, C., A Practical Guide to Splines, Springer-Verlag, 1978

8. Delvecchio, S., Dalpiaz, G., Niculita, O., Rivola, A., "Condition Monitoring in Diesel Engines For Cold Test Applications: Part I: Vibration Analysis for Pass/Fail decision", Proceedings of the 20th International Congress and Exhibitions on Condition Monitoring and Diagnostic Engineering Management (COMADEM), Faro, Portugal, 2007.

9. Fyfe, K. R. and Munck, E.D.S., "Analysis of Computed Order Tracking", Mechanical systems and Signal processing, 11(2), 1997.

10. Gagneur, J., "Improving Diesel Engine Cold Testing Diagnostic Capabilities", Diesel Progress North American Edition, Diesel and Gas Turbine Publications, Gale Group, Michigan

11. Vora, K. and Ghosh, B., "Vibration Due to Piston Slap and Combustion in Gasoline and Diesel Engines," SAE Technical Paper 911060, 1991, doi:10.4271/911060.

12. Gul, K.A., "Modeling and Analysis of Engine Cold Test Cells for Optimizing Driveline Design for Structural Reliability and Engine Assembly Defect Diagnostics", PhD Thesis, Purdue University, 2009

13. Heng, R.B.W., Nor, M. J., "Statistical Analysis of Sound and Vibration Signals for Monitoring Rolling Element Bearing Condition", Applied Acoustics, Vol. 53, No. 1-3, 1998.

14. Heywood, J.B, Internal Combustion Engine Fundamentals, McGraw-Hill, Inc., 1988.

15. Leitzinger, E.R. "Development of In-process Engine Defect Detection Methods Using NVH Indicators," Master's Thesis, University of Windsor, 2002

16. Macek, J., Polášek, M., Šika, Z., Valášek, M. et al., "Transient Engine Model as a Tool for Predictive Control," SAE Technical Paper 2006-01-0659, 2006, doi: 10.4271/2006-01-0659.

17. Martin, H.R., Honarvar, F., “Application of Statistical Moments to Bearing Failure Detection”, Applied Acoustics, Vol. 44, pp. 67-77, 1995

18. Mevel, L, Hermans, L and Van Der Auweraer, H., “Application of a subspace-based fault detection method to industrial Structures”, Mechanical Systems and Signal Processing, 13(6), 1999

19. Miller, A. J., “A New Wavelet Basis for the Decomposition of Gear Motion Error Signals and its Application to Gearbox Diagnostics”, Masters Thesis, Pennsylvania State University, 1999

20. Naber, J., Blough, J., Frankowski, D., Goble, M. et al., “Analysis of Combustion Knock Metrics in Spark-Ignition Engines,” SAE Technical Paper 2006-01-0400, 2006, doi: 10.4271/2006-01-0400.

21. Owen Owen, W., “Buick Motor Division's New Production Engine Test Facility,” SAE Technical Paper 830431, 1983, doi:10.4271/830431.

22. Pickerill, K., “Today's Technician: Automotive Engine Performance Classroom Manual 5th edition”, Delmar, Cegage Learning, 2010

23. Polonowski, C., Mathur, V., Naber, J., and Blough, J., “Accelerometer Based Sensing of Combustion in a High Speed HPCR Diesel Engine,” SAE Technical Paper 2007-01-0972, 2007, doi:10.4271/2007-01-0972.

24. Potter, R. and Gribler, M., “Computed Order Tracking Obsoletes Older Methods,” SAE Technical Paper 891131, 1989, doi:10.4271/891131.

25. Schiffbaenker, H., “Fully Automated Quality Control in Mass Production of Gasoline Engines by Means of Laser optical Vibration Measurement”, Proceedings of International Symposium on Automotive Technology and Automation, v. 1, pp 457-488.

26. Senff, F., Rußе, P., and Schlegl, T., “Genetic Algorithm-Based On-Line Optimization of a Speed Controller for a Combustion Engine,” SAE Technical Paper 2005-01-0039, 2005, doi:10.4271/2005-01-0039.

27. Tjong, J., “Engine Dynamic Signal Monitoring and Diagnostics,” PhD Thesis, University of Windsor, 1992

28. Tjong, J., Reif, Z., “Development and Applications of Engine Dynamic Signal Monitoring and Diagnostic System”, 1993.

29. Tumer, I., Huff, E.M., “Principal Component Analysis of Triaxial Vibration Data from Helicopter Transmission”, Proc. the 56th meeting of the Society of Machinery Failure & Prevention Tech., 2002.

30. Vold, H. and Deel, J., “Vold-Kalman Order Tracking: New Methods for Vehicle Sound Quality and Drive-Train NVH Applications,” SAE Technical Paper 972033, 1997, doi:10.4271/972033.

31. Wei, L., Xi, C., Jie, L., Wen, X., “Modeling and Simulation of System Dynamics for Cold Test”, Proc. 2nd Int'l Symposium on Intelligent Information Technology Application, IITA 2008, 2008.

32. Yu, K., Shi, W., Li, Y., Kong, L., “Study on the Quality Control and Management System of Engine Assembling Process”, Proc. 2009 IEEE 16th Int'l Conference on Industrial Engineering and Engineering Management, 2009.

CONTACT INFORMATION

Dr. Ienkaran Arasaratnam
Department of Mechanical Engineering
McMaster University
Hamilton, Ontario, Canada L8S 4K1
haran@ieee.org
Ph.: +1- 519-567-5738

DEFINITIONS/ABBREVIATIONS

CA
Crank Angle

CID
Cylinder IDentification

CKP
Crankshaft Position Sensor

EA-MSE
Ensemble-Averaged Mean Squared Error

ECU
Engine Control Unit

LFH
Left Front Head

LFL
Left Front Lug

LRH
Left Rear Head

LRL
Left Rear Lug

PCM
Powertrain Control Module

RFH
Right Front Head

RFL
Right Front Lug

rpm
Revolutions Per Minute

RRH
Right Rear Head

RRL
Right Rear Lug

TDC
Top Dead Center

VCT
Variable Cam Timing

VRS
Variable Reluctance Sensor

WOT
Wide Open Throttle

APPENDIX

ALGORITHM FOR COMPUTING WINDOWED-SINC INTERPOLATION

Problem Statement: Given a set of samples $\{x[i], i = 1,\ldots,m\}$ that is uniformly sampled at time $\{t[i], i = 1,\ldots,m\}$, compute a set of new sample values $\{\tilde{x}[j]\ j = 1,\ldots,n\}$ at new sampling instants $\{\tilde{t}[j], j = 1,\ldots,n\}$, where $n \geq m$

• Find the sampling period of the (old) samples:

$$t_s := (t[2] - t[1]) \tag{11}$$

• **For** $j := 1$ **To** n

$$\tilde{x}[j] := \sum_{i=1}^{m} x[i] \operatorname{sinc}\left(\frac{\tilde{t}[j] - t[i]}{t_s}\right) \tag{12}$$

End For

ISSN 0148-7191

SAE Customer Service:
Tel: 877-606-7323 (inside USA and Canada)
Tel: 724-776-4970 (outside USA)
Fax: 724-776-0790
Email: CustomerService@sae.org
SAE Web Address: http://www.sae.org
Printed in USA

SAE International